Effect of copper addition on the cluster formation behavior of Al-Mg-Si, Al-Zn-Mg and Al-Mg-Ge in the natural aging

DAICHI HATAKEYAMA, KATSUHIKO NISHIMURA, KENJI MATSUDA, TAKAHIRO NAMIKI, SEUNGWON LEE, NORIO NUNOMURA, TETSUO AIDA, TEIICHIRO MATSUZAKI, RANDI HOLMESTAD, SIGURD WENNER, and CALIN D. MARIOARA

DAICHI HATAKEYAMA, KATSUHIKO NISHIMURA, KENJI MATSUDA, TAKAHIRO NAMIKI, SEUNGWON LEE, NORIO NUNOMURA, and TETSUO AIDA are with the Graduate School of Science and Engineering, University of Toyama, Gofuku, Toyama, 930-8555, Japan

TEIICHIRO MATSUZAKI is with RIKEN Nishina Center for Accelerator Based Science, RIKEN, Wako, Saitama 351-0198, Japan

RANDI HOLMESTAD is with the Department of Physics, NTNU, Høgskoleringen 5, Trondheim NO-7491, Norway

SIGURD WENNER and CALIN D. MARIOARA are with the Materials and Chemistry SINTEF, Høgskoleringen 5, Trondheim NO-7491, Norway

*Corresponding author, E-mail: nishi@eng.u-toyama.ac.jp

Abstract

The time dependent resistivity of Al-Mg-Si(-Cu), Al-Zn-Mg(-Cu) and Al-Mg-Ge(-Cu) alloys are studied over a range of constant temperatures between 255 and 320 K. The resistivity vs. time curves for the samples show three temperature stages associated with solute element-vacancy clustering. Cu addition was found to make the stage transition time longer for the studied samples. Arrhenius plots of the transition time vs. temperature provide the activation energy (Q) of clustering from stage I to II and stage II to III. While the Cu addition increased the Q(I-II) values of Al-1.0%Mg_2Si-0.20%Cu(-0.35%Cu) and Al-2.68%Zn-3.20%Mg-0.20%Cu, it was found that the added Cu decreased the Q(I-II) value of Al-0.44%Mg-0.19Ge-0.18%Cu. The Q(II-III) values of Al-1.0%Mg_2Si and Al-2.68%Zn-3.20%Mg were slightly decreased by the Cu addition. The different effect of added Cu on the Q values is discussed in terms of diffusivity and binding energy between vacancies and solute elements.

Keywords: time dependent resistivity, Cu addition effect, clustering reaction, activation energy

1. Introduction

It is well known that the mechanical hardness of Al-Mg-Si (6xxx series) [1] and Al-Zn-Mg (7xxx series) [2] alloys are strongly related to microstructure and number densities of solute element precipitates, which are formed during natural aging (NA) and artificial aging (AA) after solution heat treatment (SHT) followed by a quick quench in water. The microstructure of the precipitates has been intensively studied via transmission electron microscopy (TEM) [3-5] and atom probe tomography (APT) [6-8] to reveal the age hardening mechanism. Differential scanning calorimetry (DSC) [9-11] has been widely used to investigate cluster formations and precipitation processes. Positron annihilation lifetime spectroscopy (PALS) [12-14] and muon spin relaxation spectroscopy (μSR) [15-17] have been used to investigate the vacancy and clustering behavior. Despite these studies, the precipitation processes, especially the early stages of clustering at NA, are still not fully understood. Recent comprehensive reviews [1, 18] of solute and trace element effects on the natural aging phenomena suggest that there are at least five stages of clustering at NA in the Al-Mg-Si alloys. The complexity of the precipitation process is due to significant sensitivity of solute clustering kinetics to the solute/trace element concentrations and NA temperatures, which dominate the duration and activation energy of each stage [1].

In the early stages of clustering, vacancies are considered to play an important role. It has been frequently observed that Cu addition to Al-Mg-Si delayed the Si/Mg-vacancy pairing and Si-complex/cluster formation (stage I) [19-21], implying that Cu has a relatively larger binding energy with vacancies in aluminum, and thus it is difficult for solute Si and Mg to cluster and bind to vacancies. In this paper, the effect of Cu addition on the activation energy for cluster formation in Al-Mg-Si(-Cu), Al-Zn-Mg(-Cu) and Al-Mg-Ge(-Cu) alloys is reported via electrical resistivity measurements. The findings are discussed by considering the diffusivity of solute elements and Cu-vacancy binding energy.

2. Experimental Procedure

The materials used in this study were prepared by melting pure Al (purity, 99.99 %) with Si and Mg (purity, 99.9 %), Cu and Zn (purity, 99.99 %) in air. The resulting ingots were formed into 2.0 mm thick plates by hot and cold rolling. Several pieces of the samples were cut out from the plate with the approximate dimensions of $1.0 \times 2.0 \times 30.0$ mm^3. The chemical compositions, sample notations, and heat treatment temperatures are described in Table 1. Four Pt wires were welded on the samples for resistivity measurements. The samples were annealed at 848/753/873 K for 1 hour

solution heat treatment and directly quenched into ice-water (SHTQ). The samples were set on the sample holder of an electrical resistivity measurement system within five minutes after quenching. The time dependent resistivity was continuously measured using a DC current of 100 mA, with the samples maintained at a constant temperature between 255 and 330 K for a few days.

3. Results

Figure 1 shows the time variation of resistivity (ρ) of Mg2Si02Cu at 300 K. The horizontal axis denotes the time (t) from SHTQ on a logarithmic scale. It is clear that ρ varies, firstly in an increasing rate (concave shape), then later in a decreasing rate (convex shape) from around 10^3 minutes. Similar time variations are often observed in ternary and quaternary aluminum alloys but not observed in pure aluminum or binary Al-Si/Al-Mg aluminum alloys (see supplement). Banhart et al. assigned four clustering stages (stage I ~ IV) to the time variation of ρ in Al-Mg-Si alloys from PALS and ρ measurements [18]. The time variation of ρ in Figure 1 is corresponding well to their assignment for the stages I, II and III. For quantitative discussions, we adopted their method to evaluate the stage transition time; the data points up to 250 minutes were fit with a linear function, those from 250 to 1100 minutes and from 1100 to 4000 minutes were fit with logarithmic functions: $\rho = \rho_0 + \rho^* \log(t)$, ($\rho^*$ is defined as a resistivity change coefficient in this paper). The arrows in Figure 1 indicate the intersections of the fitted functions, which are considered to be the stage boundaries.

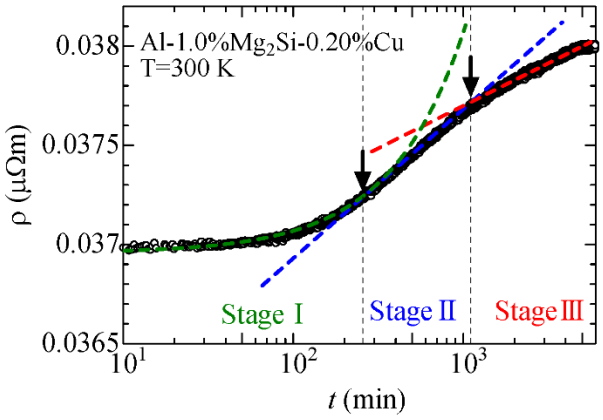

Figure 1. Time dependence of electrical resistivity of an Al-1.0%Mg_2Si-0.20%Cu alloy at 300 K. The times that the electrical resistivity changes occur are marked by the arrows which were determined as the intersection points of the two least-square fits.

The time dependence of ρ in Mg2Si was measured in an isothermal condition with a temperature

between 255 and 300 K. The results of the measurements are shown in Figure 2(a), in which the solid lines present the ρ changes ($\Delta\rho = \rho - \rho_0$, ρ_0: an averaged value at the beginning) obtained by a least square fit of the data to a ninth degrees polynomial function. All lines increased with time. The stage transition time, at which ρ started to increase, was clearly delayed at the lower temperatures. Once ρ increased, however, the increasing rate of ρ was larger at the lower temperatures, and Δρ at 255 K seems to be maximum among the data lines in Figure 2(a). The Δρ vs. *t* for Mg2Si02Cu is presented in Figure 2(b). Over all appearances of the fitted lines are similar to those in Figure 2(a), except for the measuring temperature range which is approximately 30 K higher. A comparison of Δρ in Mg2Si, Mg2Si02Cu and Mg2Si035Cu at 280 K is given in Figure 3, in which it can be seen that the Cu addition clearly prolonged the stage transition time. The arrows in Figure 3 are the results of the fitting as explained in Figure 1, corresponding to the transition time from the stage I to II, (t_{I-II}). Further, the stage transition time of Mg2Si035Cu was longer than that of Mg2Si02Cu. There are a plenty of studies reporting similar Cu addition effect on the stage transition time [1, 21].

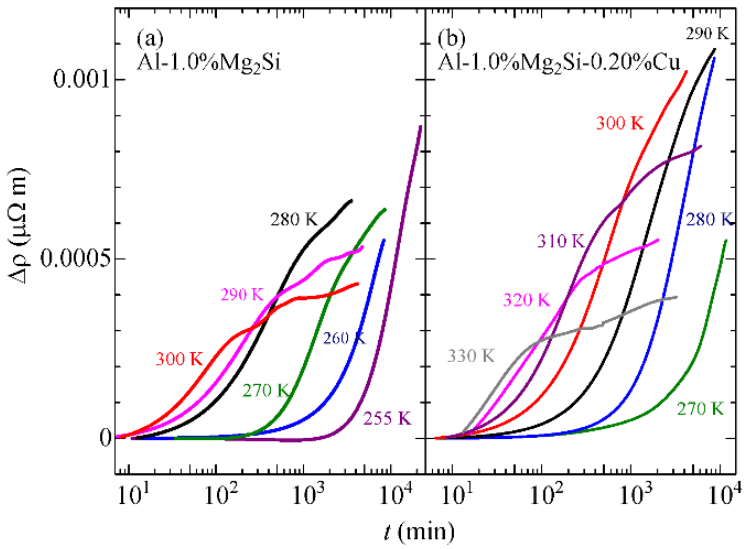

Figure 2. Time dependence of electrical resistivity changes of (a) Al-1.6%Mg_2Si alloy and (b) Al-1.0%Mg_2Si-0.20%Cu at a constant temperature between 255 and 330K.

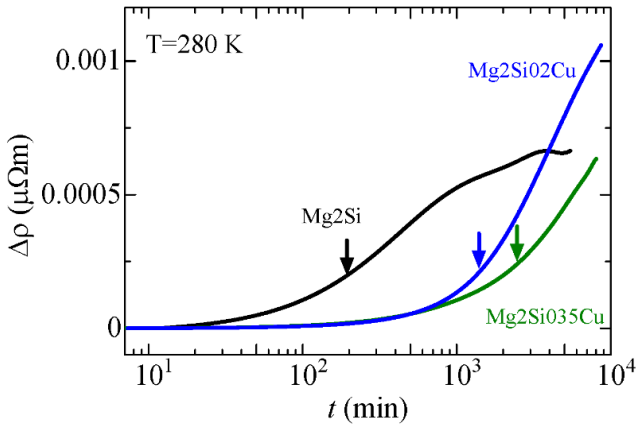

Figure 3. A comparison of the time dependence of electrical resistivity changes of Al-1.0%Mg_2Si, Al-1.0%Mg_2Si-0.20%Cu and Al-1.0%Mg_2Si-0.35%Cu [22]at 280 K.

Figures 4(a) and 4(b) show Δρ vs. *t* for ZnMg and ZnMg02Cu, respectively, at temperatures from 260 to 320 K. It is found that the same explanation as that given for Mg2Si and Mg2Si02Cu is valid for ZnMg and ZnMg02Cu, indicating that t_{I-II} was delayed by the Cu addition. Figures 5(a) and 5(b) show Δρ vs. *t* for MgGe and MgGe02Cu, respectively. It is worth mentioning that the transition time from stage I to II for MgGe is noticeable even at 320 K in Figure 5(a), where Δρ values at 320 K were reduced by half for drawing. Some of the ρ values decreased with time in the early NA period. This different variation of Δρ vs. *t* between Al-Mg-Si(-Cu) and Al-Mg-Ge(-Cu) is possibly ascribed to the different diffusivity of Si and Ge. Addition of Cu to MgGe further prolonged the stage transition time as seen in Figure 5(b). The magnitude of Δρ in MgGe is larger than that in MgGe02Cu for the later NA periods. This is opposite to those in Al-Mg-Si(-Cu) and Al-Zn-Mg(-Cu).

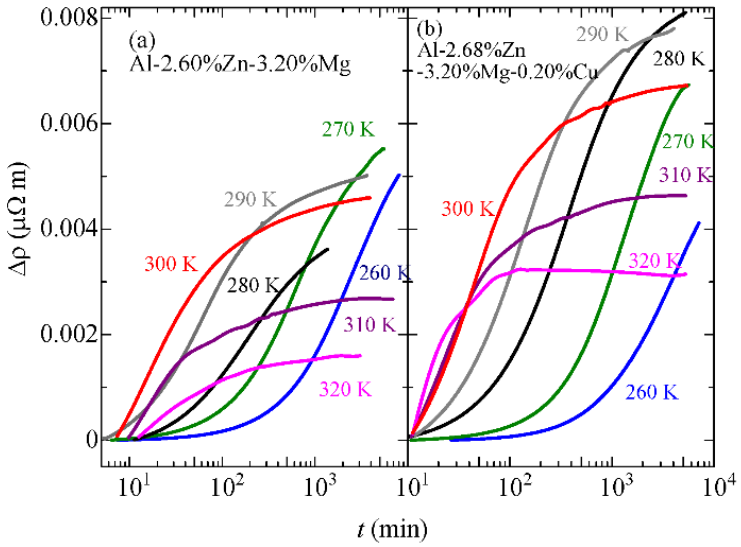

Figure 4. Time dependence of electrical resistivity changes of (a) Al-2.60%Zn-3.20%Mg and (b) Al-2.68%Zn-3.20%Mg-0.20%Cu at a constant temperature between 260 and 320K.

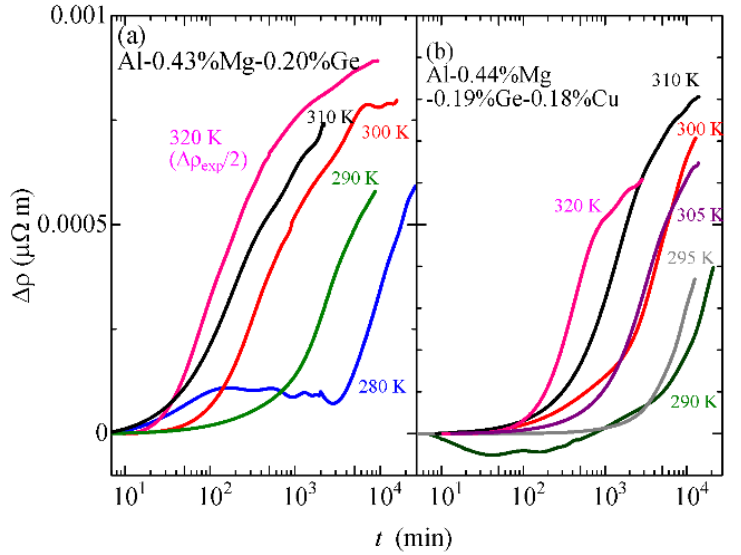

Figure 5. Time dependencies of electrical resistivity changes of (a) Al-0.43%Mg-0.20%Ge and Al-0.44%Mg-0.19%Ge-0.18%Cu at a constant temperature between 280 and 320K.

4. Discussions

The time dependence of ρ in the present samples indicated that the Cu addition delayed the transition between stages I and II. In the initial clustering stage after SHTQ, quenched-in excess

vacancies were caught by Cu atoms, so Si/Zn/Ge atoms were slow to make Si/Zn/Ge-vacancy pairs and complexes (stage I), consequently the Si/Zn/Ge-rich clustering (stage II) was prolonged. This interpretation is supported by the fact that a larger amount of added Cu made a longer delaying effect on the stage transition time as shown in Figure 3.

Figure 6(a) shows the resistivity change coefficient (ρ*) in stage II of Mg2Si, Mg2Si02Cu and Mg2Si035Cu, calculated from the data in Figures 2(a) and 2(b), plus the data in reference [22]. The ρ* are larger at lower NA temperatures. This can be ascribed to the large number density of small sized clusters; the slow clustering due to a low temperature resulted in small Si-rich clusters [21]. It is interesting that the ρ* data points for Mg2Si almost overlap with those of Mg2S02Cu and Mg2Si035Cu if they are shift toward the high temperature side by roughly 30 K. This finding implies that the added Cu atoms mainly interacted with vacancies, but did not significantly affect the Si-rich clustering in the stage II.

The ρ* values for ZnMg and ZnMg02Cu in Figure 6(b) are approximately an order of magnitude larger than those in Figure 6(a), due to the high Zn and Mg concentrations. The Cu addition definitely increased the ρ* further, but the NA temperature dependence is unclear. The Cu addition effect on the ρ* for Al-Mg-Ge in Figure 6(c) was found to be different from those for Al-Mg-Si and Al-Zn-Mg as the Cu addition did not always increase the ρ* values.

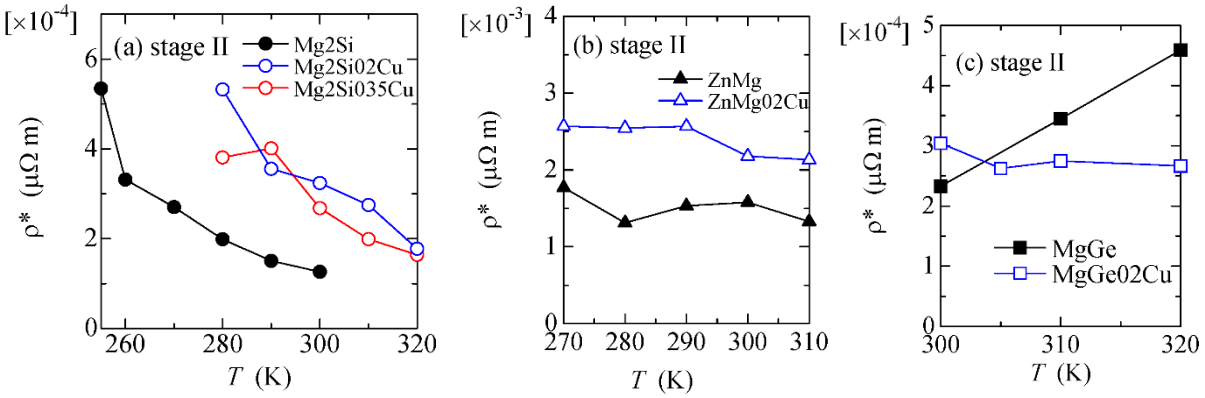

Figure 6. Comparison of the resistivity change coefficients of (a) Al-Mg-Si(-Cu), (b) Al-Zn-Mg(-Cu), and (c) Al-Mg-Ge(-Cu) samples in the clustering stage II.

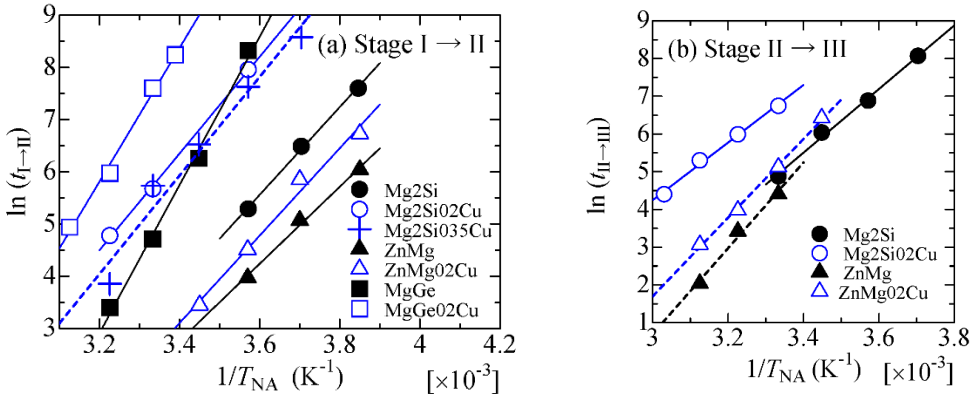

Figure 7 Arrhenius plots for (a) Al-Mg-Si(-Cu), Al-Zn-Mg(-Cu), and Al-Mg-Ge(-Cu) using the transition times from stage I to II, and (b) Al-Mg-Si(-Cu) and Al-Zn-Mg(-Cu) using the transition times from stage II to III, and natural aging temperatures.

For more quantitative discussions about the Cu addition effect, the activation energies for cluster formation (Q) were extracted from the stage transition times. Figures 7(a) (stage I - II) and 7(b) (stage II - III) present Arrhenius plots of the logarithmic transition time against reciprocal temperature of NA, $\ln(t) \sim Q/k_B T_{NA}$, based on the data in Figures 2 ~ 5 and in reference [22]. Least square fits of the data yield the activation energy, as drawn in Figures 8 and 9 for the stage I - II and stage II - III, respectively. In Figure 8, the Q values were increased by the Cu addition for Al-Mg-Si and Al-Zn-Mg in the transition between stage I and II. The Cu addition for Al-Mg-Ge, however, decreased the Q value in the same transition. Further, in the stage transition II - III, Cu additions in Al-Mg-Si and Al-Zn-Mg gave a small decrease in the Q values.

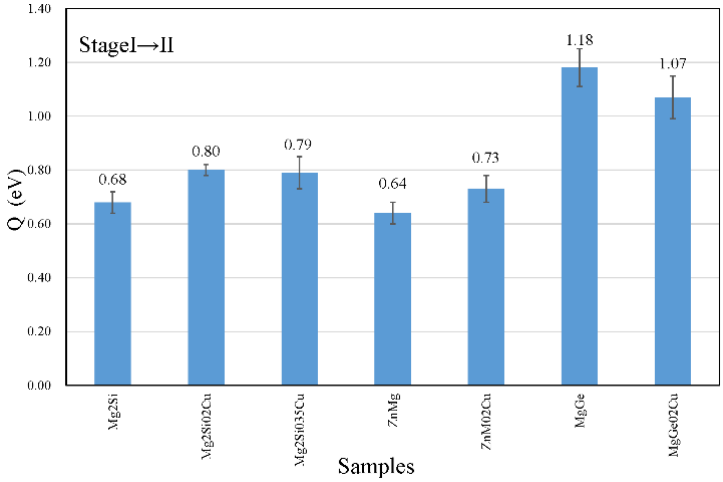

Figure 8 Activation clustering energy Q estimated from the Arrhenius plots in Figure 7(a).

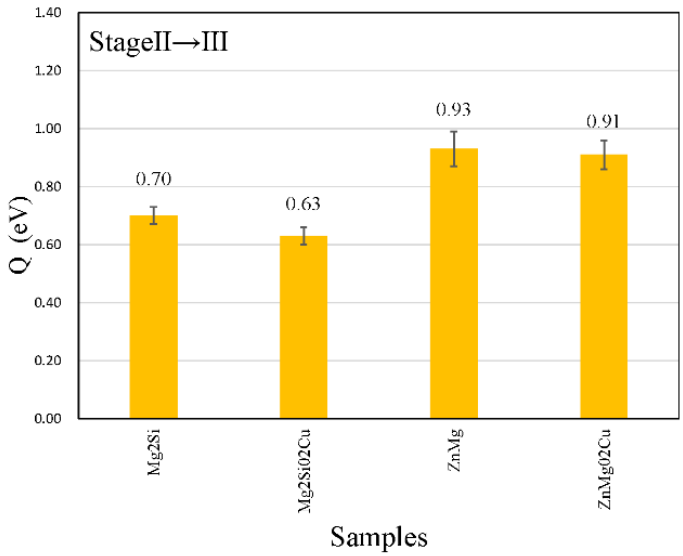

Figure 9 Activation clustering energy *Q* estimated from the Arrhenius plots in Figure 7(b).

The observed trends in the *Q* values by Cu additions most likely result from the vacancy behavior. Recent density functional theory calculations [21, 23-25] provide the solute-vacancy binding energies (*E*), for Si, Zn, Mg, Cu, and Ge atoms to be *E*(Si-V) = 0.033, *E*(Zn-V) = 0.032, *E*(Mg-V) = 0.026, *E*(Cu-V) = 0.124 and *E*(Ge-V) = 0.053 eV, respectively. As seen, the binding energy of Cu-vacancy is the largest among the present solute elements. Concerning the diffusivity (*D*), of the solutes, it is generally postulated that Si and Zn diffuse relatively fast with the aid of vacancies in aluminum, but Mg, Ge and Cu are slow to move at a natural aging temperature. A tentative estimation using the parameters for the *D* values [26] yield *D*(Si) ~5 x 10^{-26}, *D*(Zn) ~ 7 x 10^{-26}, *D*(Mg) ~ 2 x 10^{-26}, *D*(Ge) ~ 4 x 10^{-26} and *D*(Cu) ~ 2 x 10^{-28} m^2/s in aluminum at 300 K, tells that the *D*(Cu) value is two orders of magnitude smaller than the others. The solute elements need vacancies to move and form clusters. Immediately after SHTQ, excess vacancies of approximately 100 ppm are considered to be present in aluminum alloys. This concentration is about one hundredth of the solutes. A part of the vacancies will form solute-vacancy pairs, and others will be absorbed in lattice imperfections such as grain boundaries, dislocation loops and impurities.

Based on this Si-vacancy and Mg-vacancy pairs are produced first in Mg2Si after SHTQ. During NA in stage I, a mobile Si-vacancy pair will encounter other Si-vacancy pairs, starting to form mobile Si complexes of a few Si atoms, releasing a part of vacancies, which leads to new solute-vacancy pair formations. As the Si complexes grow larger in size and become clusters, the vacancies will have difficulties to escape from the clusters [27]. Consequently, at the end of stage I, a part of quenched-in vacancies is either trapped in the clusters or lost at imperfections. Since the Mg-vacancy pairs move slowly, formation of Mg containing Si complexes proceeds in a slow rate.

Once stage I ends, however, the Mg-vacancy pairs play an important role to grow clusters and release vacancies to transport solute atoms. This scenario can also be valid in the clustering process for Al-Zn-Mg, since Zn-vacancy pairs move fast.

Since a Cu-vacancy pair has large binding energy and a relatively small diffusion rate, formation of Si complexes in the Cu-added alloys during NA in stage I will proceed at a slower rate than in the Cu-free alloys, due to the lower number density of Si(Zn)-vacancy pairs, leading to the larger *Q*(I-II) values. The DSC study by Chang et al. [28] reported that the *Q*(I-II) values mainly depended on the Si concentrations in Al-Mg-Si alloys. At the end of stage I, a large number density of small Si(Zn) clusters is therefore expected. Since the distance between small solute clusters in the Cu-added alloys is shorter than in the Cu-free ones, the Mg-vacancy pairs can relatively easily encounter Si(Zn) clusters. Thus, the cluster formation is accelerated, resulting in the smaller *Q* values from stage II to III for the Cu-added alloys.

For the Al-Mg-Ge(-Cu)alloys, we see that these three solutes have smaller diffusivity than those of Si and Zn in NA, which can be responsible to the largest *Q*(I-II) value of MgGe. The stage transition time from stage I to II was definitely longer in MgGe02Cu, due to the Cu addition effect, however, the deduced *Q*(I-II) value is smaller than that in MgGe. This is opposite to the Al-Mg-Si(-Cu) and Al-Zn-Mg(-Cu) cases. In the stage I, Ge-vacancy pair and Ge complex formations proceed for a long period, during which vacancies were trapped in Ge complexes or lost in imperfections. Since the solute concentration of Ge(Cu) is larger in MgGe02Cu than that in MgGe, we expect a larger number of solute-vacancy pairs in MgGe02Cu. The larger number of vacancies can facilitate clustering and make the *Q*(I-II) value in MgGe02Cu smaller.

5. Conclusion

Time-dependent resistivity measurements of Al-Mg-Si(-Cu), Al-Zn-Mg(-Cu) and Al-Mg-Ge(-Cu) alloys have been carried out at constant temperatures between 255 and 320 K. The effect of Cu additions on the stage transition time has been evaluated, which enable quantitative discussions about cluster activation energies. From the present study three conclusions can be drawn;

1. Cu additions in Al-1.0%Mg_2Si, Al-2.68%Zn-3.20%Mg, and Al-0.44%Mg-0.19%Ge prolonged the stage transition time from stage I to II, due to the strong binding energy between Cu and vacancy, resulting in fewer vacancies available for solute atoms to diffuse in aluminum.
2. The Cu addition was found to increase the activation energy from stage I to II for Al-1.0%Mg_2Si and Al-2.68%Zn-3.20%Mg, but decrease the activation energy from stage II to III. The slow clustering in stage I led to a large number density of small sized Si or Zn clusters, which accelerate the Si(Zn)-Mg co-clustering in stage II.

3. It was found that the Cu addition to Al-0.44%Mg-0.19%Ge prolonged the stage transition time of stage I, but decreased the activation energy in the same stage. The small diffusivity of both Ge and Cu made the stage transition time quite long in stage I, but the number of vacancies was kept relatively large due to Cu atoms, which additionally facilitated the Ge clustering.

Acknowledgments

This study has been supported by the funds from Center for Advanced Materials Research and International Collaboration, University of Toyama, The Norwegian-Japanese Aluminium alloy Research and Education Collaboration (INTPART), project number 249698, and The Japan Institute of Light Metals.

References:

[1] M. Werinos, H. Antrekowitsch, T. Ebner, R. Prillhofer, P.J. Uggowitzer, and S. Pogatscher：*Mater. Des.*, 2016, vol.107, pp. 257-268.

[2] S.K. Maloney, K Hono, I.J. Polmear, and S.P. Ringer: *Micron*,2001, vol. 32, pp. 741-747

[3] Y. Weng, Z. Jia, L. Ding, Y. Pan, Y. Liu, and Q. Liu：*J. Alloy. Compd.*, 2017, vol. 695, pp. 2444-2452.

[4] Q. Xiao, H. Liu, D. Yi, D. Yin, Y. Chen, Y. Zhang, and B. Wang：*J. Alloy. Compd.*, 2017, vol. 695, pp. 1005-1013.

[5] K. Matsuda, A. Kawai, K. Watanabe, S. Lee, C. D. Marioara, S. Wenner, K. Nishimura, T. Matsuzaki, N. Nunomura, T. Sato, R. Holmestad, and S. Ikeno: *Mater. Trans.* 2017, vol. 56, pp. 167-175

G.Tao, C.Liu, J.Chen, Y.Lai, P.Ma and L.Liu：Mater. Sci. Eng., *A*, 2015, vol. 642, pp. 241-248.

[6] A. Serizawa, S. Hirosawa, and T. Sato: *Metall. Mater. Trans., A*, 2008, vol. 39, pp. 243-251.

[7] Y. Aruga, M. Kozuka, Y. Takaki, and T. Sato：*Scr. Mater.*, 2016, vol. 116, pp. 82-86.

[8] M. Murayama and K. Hono: *Acta Mater.*, 1999, vol. 47, pp. 1537-1548.

[9] C.S.T. Chang and J. Banhart：*Matal. Mater. Trans*., *A*, 2011, vol. 42, pp. 1960-1964.

[10] J.H. Kim, E. Kobayashi, and T. Sato：*Mater. Trans.*, 2011, vol. 52, pp. 906-913.

[11] L. Ding, Z. Jia, Y. Liu, Y. Weng, and Q. Liu：*J. Alloy. Compd.*, 2016, vol. 688, pp. 362-367.

[12] M. Liu, B. Klobes, and J. Banhart: *Mater. Sci.*, 2016, vol. 51, pp. 7754-7767.

[13] J. Banhart, M.D. H.Lay, C.S.T. Chang, and A.J. Hill: *Phys. Rev. B*, 2011, vol. 83, pp. 014101-014113.

[14] M.D. H.Lay, H.S. Zurob, C.R. Hutchinson, T.J. Hill, and A.J. Hill：*Metal. Mater. Trans., A*, 2012, vol. 43, pp. 4507-4513.

[15] S. Wenner, R. Holmestad, K. Matsuda, K. Nishimura, T. Matsuzaki, D. Tomono, F.L. Platt, and C.D. Marioara：*Phys. Rev. B*, 2012, vol. 86, pp. 014201-014207.

[16] S. Wenner, K. Nishimura, K. Matsuda, T. Matsuzaki, D. Tomono, F.L. Platt, C.D. Marioara, and R. Holmestad：*Acta Mater*., 2013, vol. 61, pp. 6082-6092.

[17] K. Nishimura, K. Matsuda, R. Komaki, N. Nunomura, S. Wenner, R. Holmestad, T. Matsuzaki, I. Watanabe, F.L. Pratt, and C.D. Marioara: *J. Phys. Conf. Ser*., 2014, vol. 551, 012031.
[18] J. Banhart, C.S.T. Chang, Z. Liang, N. Wanderka, M.D. H.Lay, and A.J. Hill: *Adv. Eng. Mater.*, 2010, vol. 7, pp. 559-571.
[19] J.H. Kim, H. Tezuka, E. Kobayashi, and T. Sato：*Kor. J.Mater. Res.*, 2012, vol. 22, pp. 329-334.
[20] M.W. Zandbergen, A. Cerezo, and G.D. W.Smith：*Acta Mater.*, 2015, vol. 101, pp. 149-158.
[21] M. Liu and J. Banhart: *Mater. Sci. Eng. A*, 2016, vol. 658, pp. 238-245.
[22] D. Hatakeyama, K. Nishimura, T. Namiki, K. Matsuda, N. Nunomura and T. Matsuzaki：Japan Institute of Light Metals, 2017, vol. 67, pp. 168-172. (in Japanese)
[23] P. Lang, Y.V. Shan, and E. Kozeschnik：*Mater. Sci. Forum*, 2014, vols.794-796, pp. 963-970.
[24] P. Lang, T. Weisz, M.R. Ahmadi, E. Povoden-Karadeniz, A. Falahati, and E. Kozeschnik：*Adv. Mater. Res.*, 2014, vol. 922, pp. 406-411.
[25] C. Worverton：*Acta Mater.*, 2007, vol. 55, pp. 5867-5872.
[26] Y. Du, Y. A. Chang, B. Huang, W. Gong, Z. Jin, H. Xu, Z. Yuan, Y. Liu, Y. He, F.-Y. Xie: *Mater. Sci. Eng. A* 2003, vol. 363, pp. 140-151
[27] H.S. Zurob and H. Seyedrezai: *Scr. Mater.*, 2009, vol. 61, pp. 141-144.
[28] C. S. T Chang, Z. Liang, E. Schmidt, and J. Banhart: *Int. J. Mat Res.* 2012, vol. 103, pp. 955-961

List of figure captions

Figure 1. Time dependence of electrical resistivity of an Al-1.0%Mg_2Si-0.20%Cu alloy at 300 K. The times that the electrical resistivity changes occur are marked by the arrows which were determined as the intersection points of the two least-square fits.

Figure 2. Time dependence of electrical resistivity changes of (a) Al-1.6%Mg_2Si alloy and (b) Al-1.0%Mg_2Si-0.20%Cu at a constant temperature between 255 and 330K.

Figure 3. A comparison of the time dependence of electrical resistivity changes of Al-1.0%Mg_2Si, Al-1.0%Mg_2Si-0.20%Cu and Al-1.0%Mg_2Si-0.35%Cu [22]at 280 K.

Figure 4. Time dependence of electrical resistivity changes of (a) Al-2.60%Zn-3.20%Mg and (b) Al-2.68%Zn-3.20%Mg-0.20%Cu at a constant temperature between 260 and 320K.

Figure 5. Time dependencies of electrical resistivity changes of (a) Al-0.43%Mg-0.20%Ge and Al-0.44%Mg-0.19%Ge-0.18%Cu at a constant temperature between 280 and 320K.

Figure 6. Comparison of the resistivity change coefficients of (a) Al-Mg-Si(-Cu), (b) Al-Zn-Mg(-Cu), and (c) Al-Mg-Ge(-Cu) samples in the clustering stage II.

Figure 7 Arrhenius plots for (a) Al-Mg-Si(-Cu), Al-Zn-Mg(-Cu), and Al-Mg-Ge(-Cu) using the transition times from stage I to II, and (b) Al-Mg-Si(-Cu) and Al-Zn-Mg(-Cu) using the transition times from stage II to III, and natural aging temperatures.

Figure 8 Activation clustering energy *Q* estimated from the Arrhenius plots in Figure 7(a).

Figure 9 Activation clustering energy *Q* estimated from the Arrhenius plots in Figure 7(b).

Table1 Sample composition of studied alloys, sample notation labels, and solution heat treatment (SHT) temperature.

Sample composition [at.%]	Notation	SHT temp. [K]
Al-1.0%Mg2Si	Mg2Si	
Al-1.0%Mg2Si-0.20%Cu	Mg2Si02Cu	848
Al-1.0%Mg2Si-0.35%Cu	Mg2Si035Cu	
Al-2.60%Zn-3.20Mg	ZnMg	753
Al-2.68%Zn-3.20%Mg-0.20%Cu	ZnMg02Cu	
Al-0.43%Mg-0.20%Ge	MgGe	873
Al-0.44%Mg-0.19%Ge-0.18%Cu	MgGe02Cu	

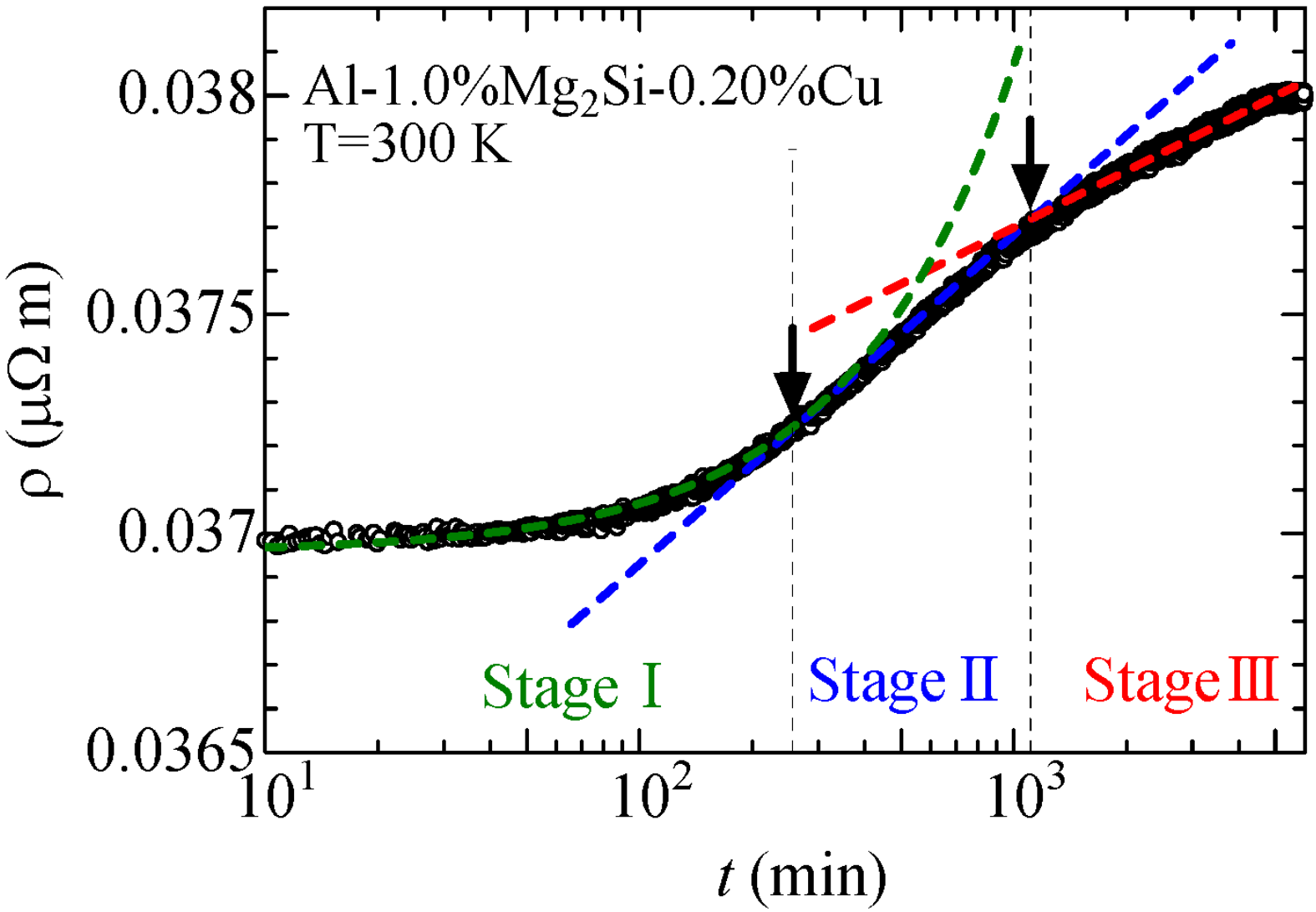
Al-1.0%Mg2Si-0.20%Cu
T=300 K
0.038
0.0375
0.037
0.0365
ρ (μΩ m)
10^1
10^2
10^3
t (min)
Stage I
Stage II
Stage III

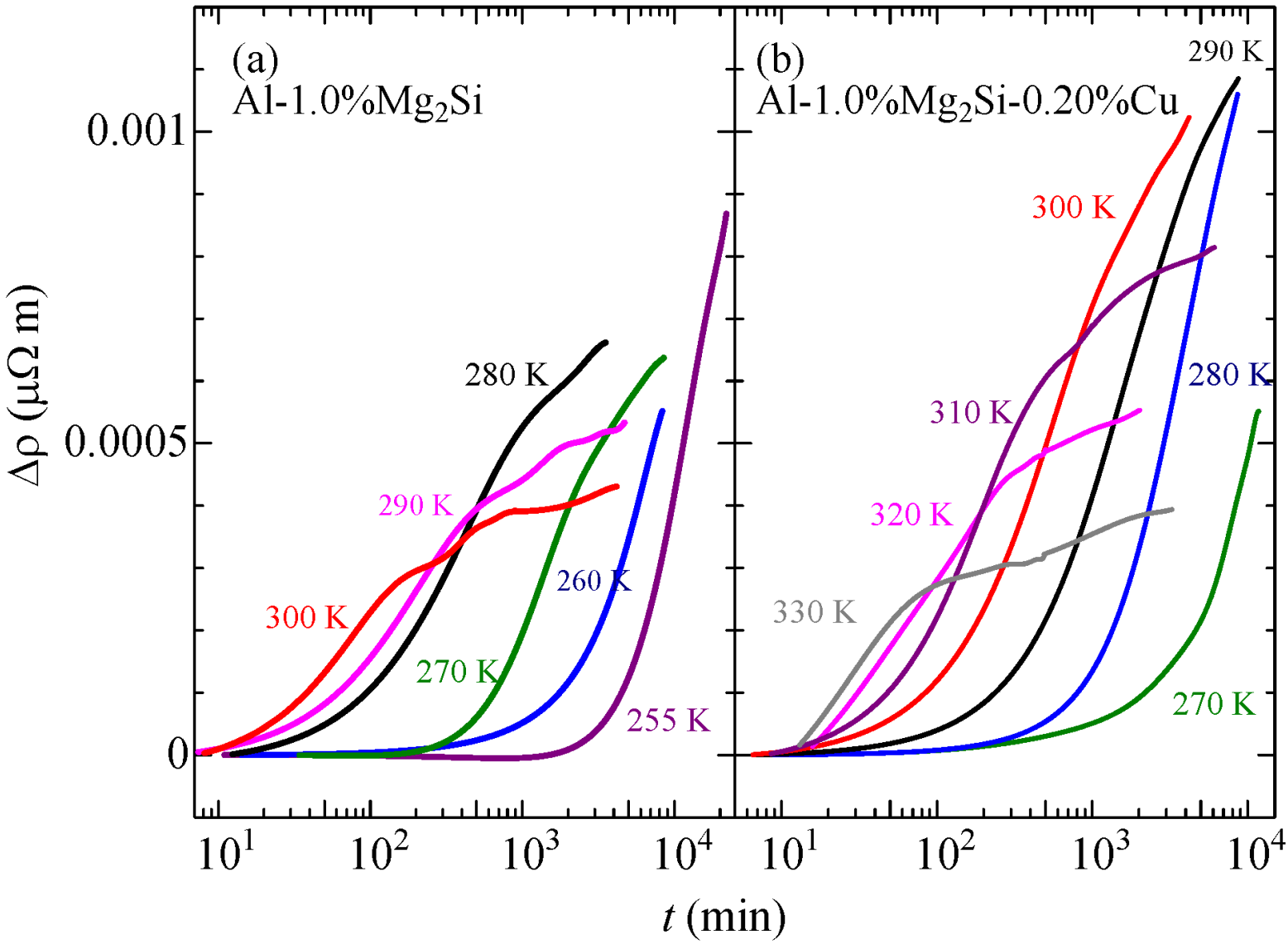
(a)
Al-1.0%Mg2Si
(b)
Al-1.0%Mg2Si-0.20%Cu
Δρ (μΩ m)
0.001
0.0005
0
280 K
290 K
300 K
260 K
270 K
255 K
290 K
300 K
310 K
280 K
320 K
330 K
270 K
10^1
10^2
10^3
10^4
t (min)

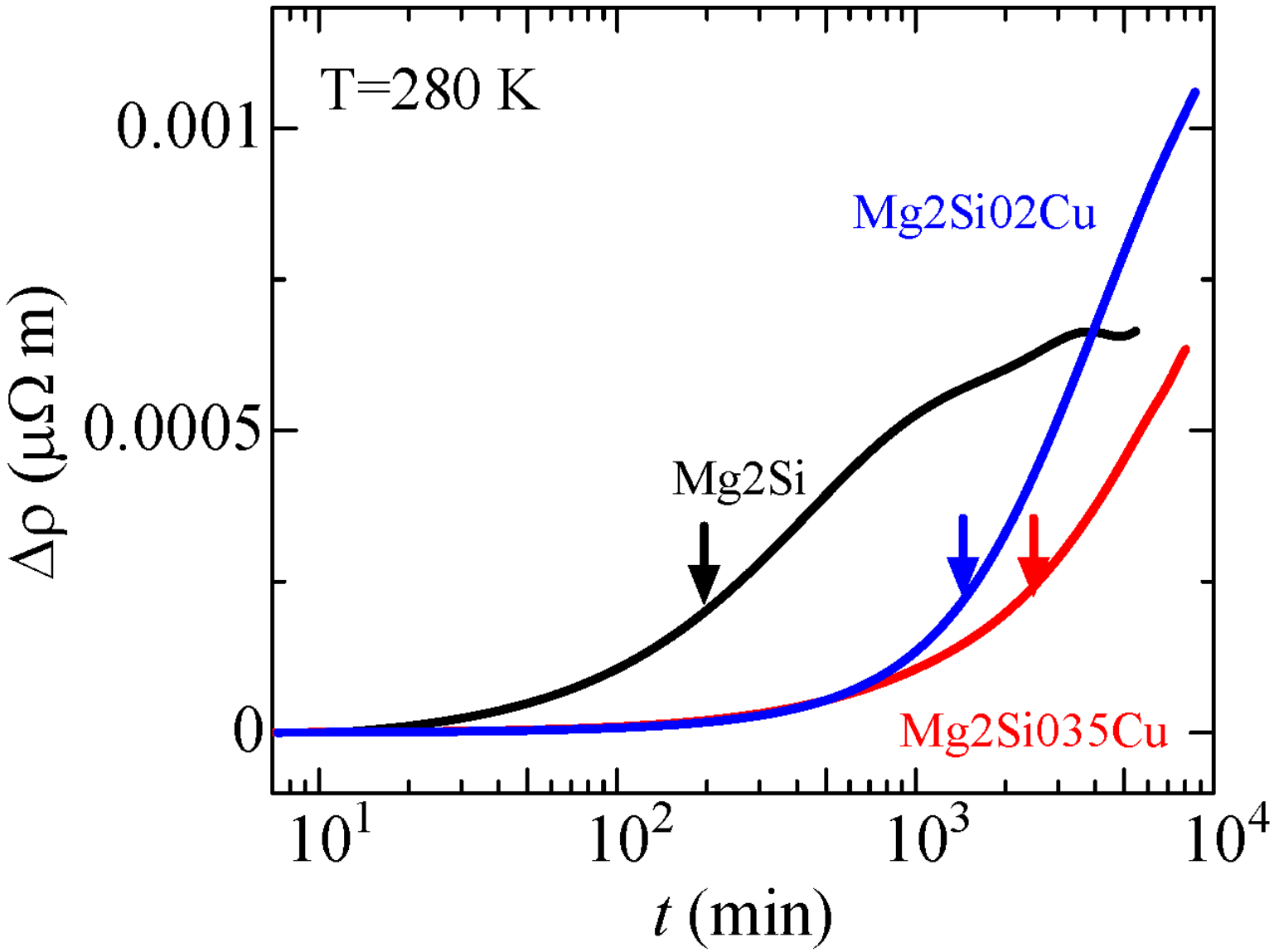
T=280 K
0.001
0.0005
0
Δρ (μΩ m)
Mg2Si02Cu
Mg2Si
Mg2Si035Cu
10^1
10^2
10^3
10^4
t (min)

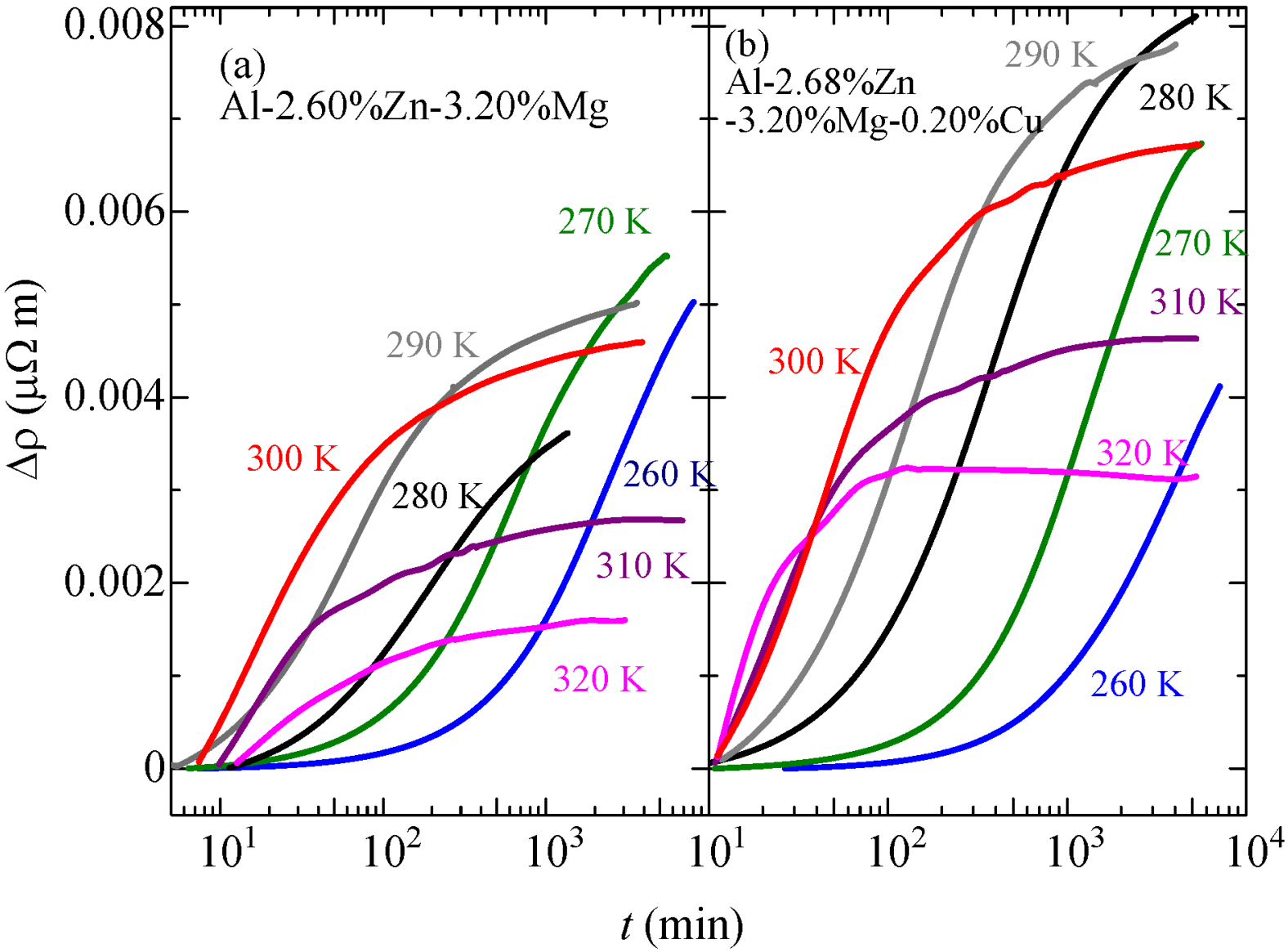
(a)
Al-2.60%Zn-3.20%Mg
(b)
Al-2.68%Zn
-3.20%Mg-0.20%Cu
0.008
0.006
0.004
0.002
0
Δρ (μΩ m)
290 K
280 K
270 K
300 K
260 K
310 K
320 K
10^1
10^2
10^3
10^4
t (min)

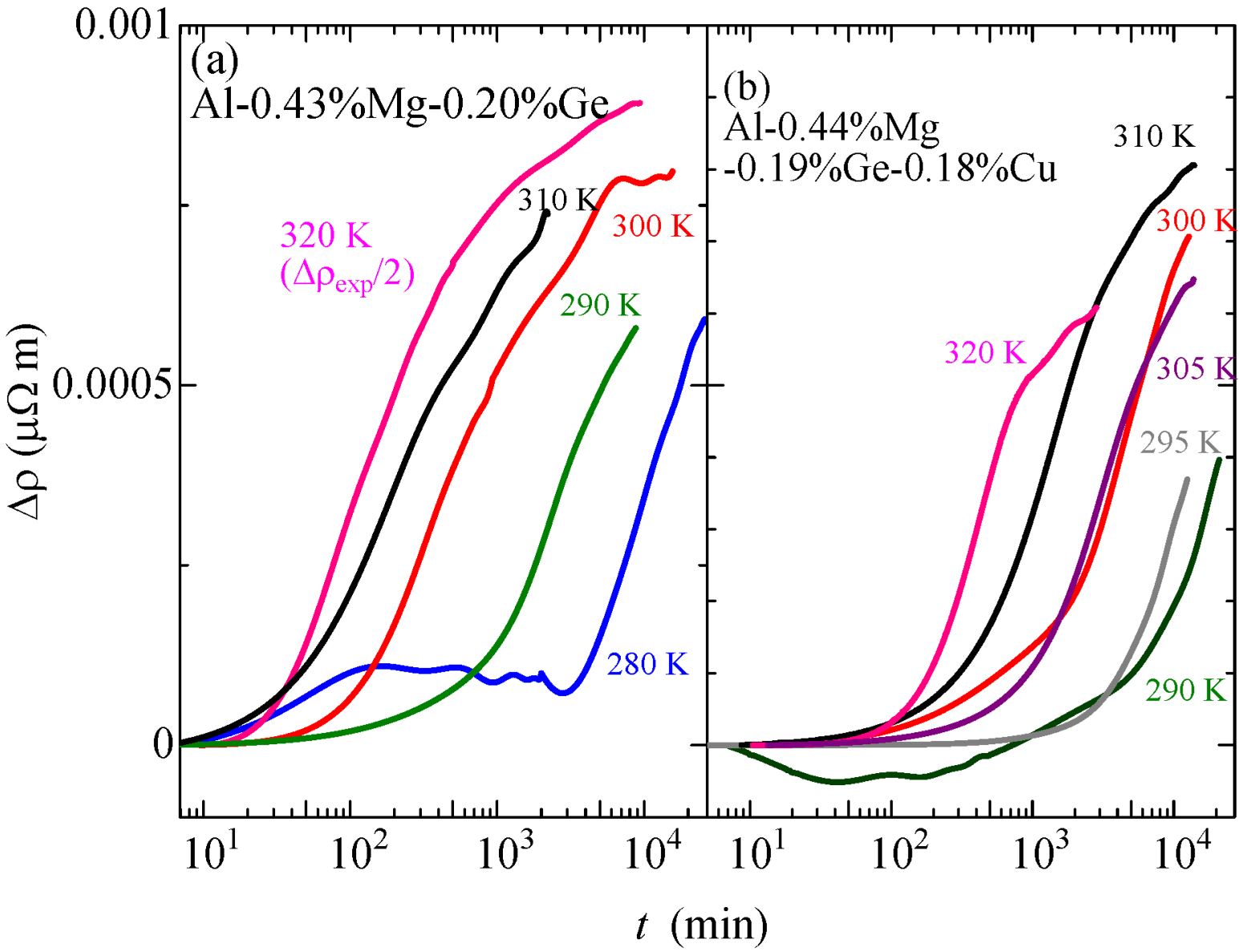
0.001
0.0005
0
Δρ (μΩ m)
(a)
Al-0.43%Mg-0.20%Ge
320 K
(Δρexp/2)
310 K
300 K
290 K
280 K
(b)
Al-0.44%Mg
-0.19%Ge-0.18%Cu
310 K
300 K
320 K
305 K
295 K
290 K
10^1
10^2
10^3
10^4
t (min)

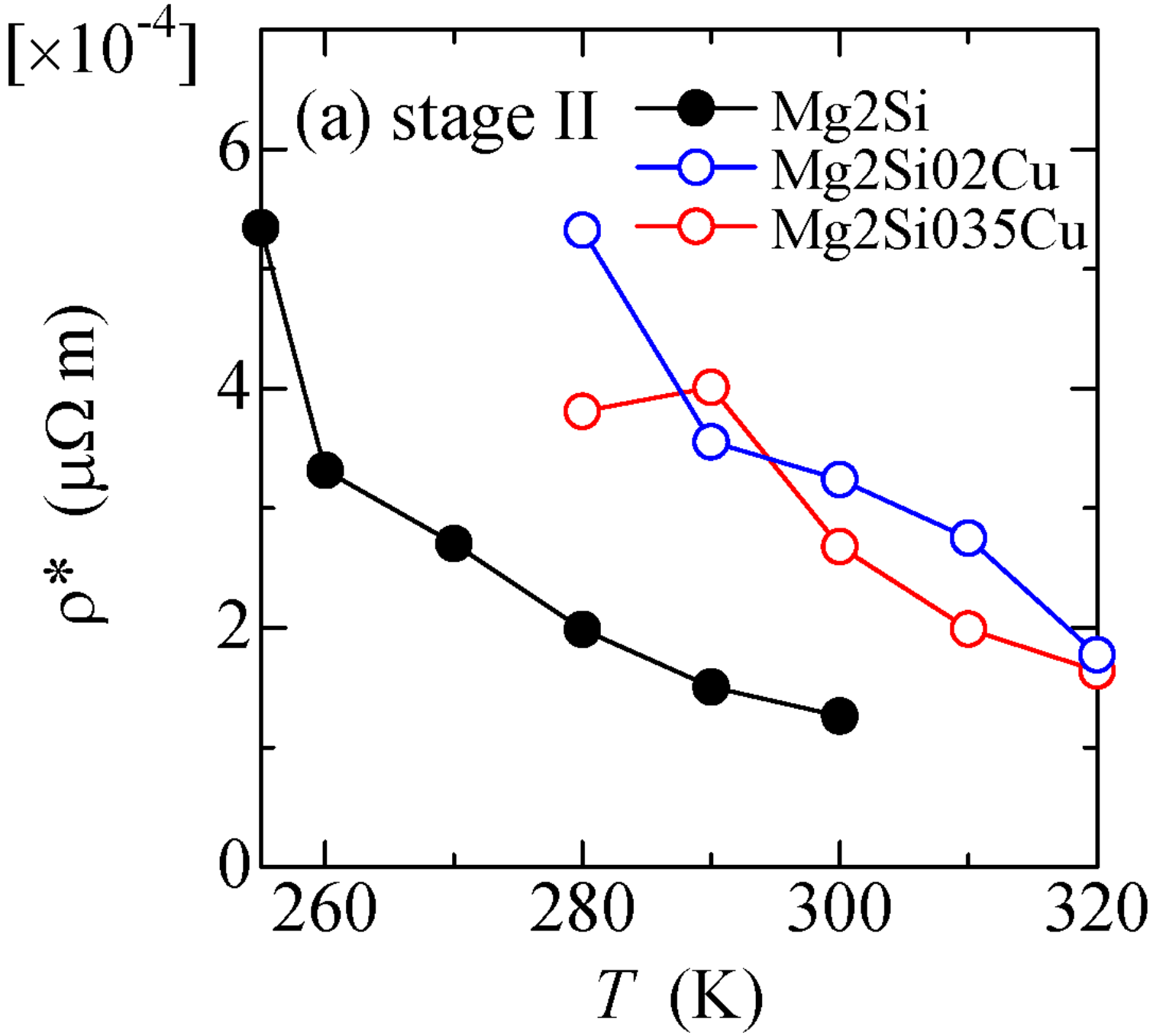
[×10-4]
(a) stage II
Mg2Si
Mg2Si02Cu
Mg2Si035Cu
ρ* (μΩ m)
6
4
2
0
260
280
300
320
T (K)

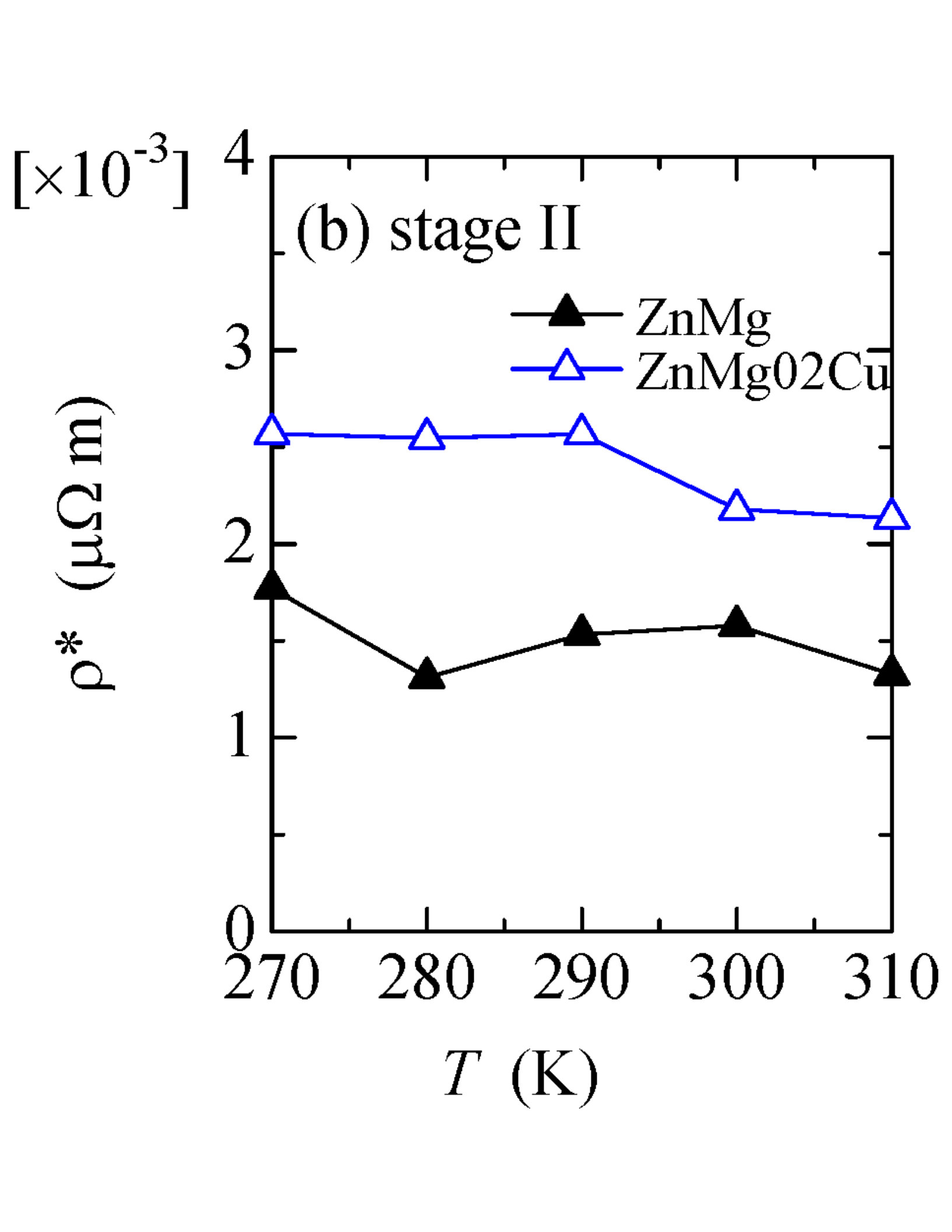
[×10-3]
4
3
2
1
0
(b) stage II
ZnMg
ZnMg02Cu
ρ* (μΩ m)
270
280
290
300
310
T (K)

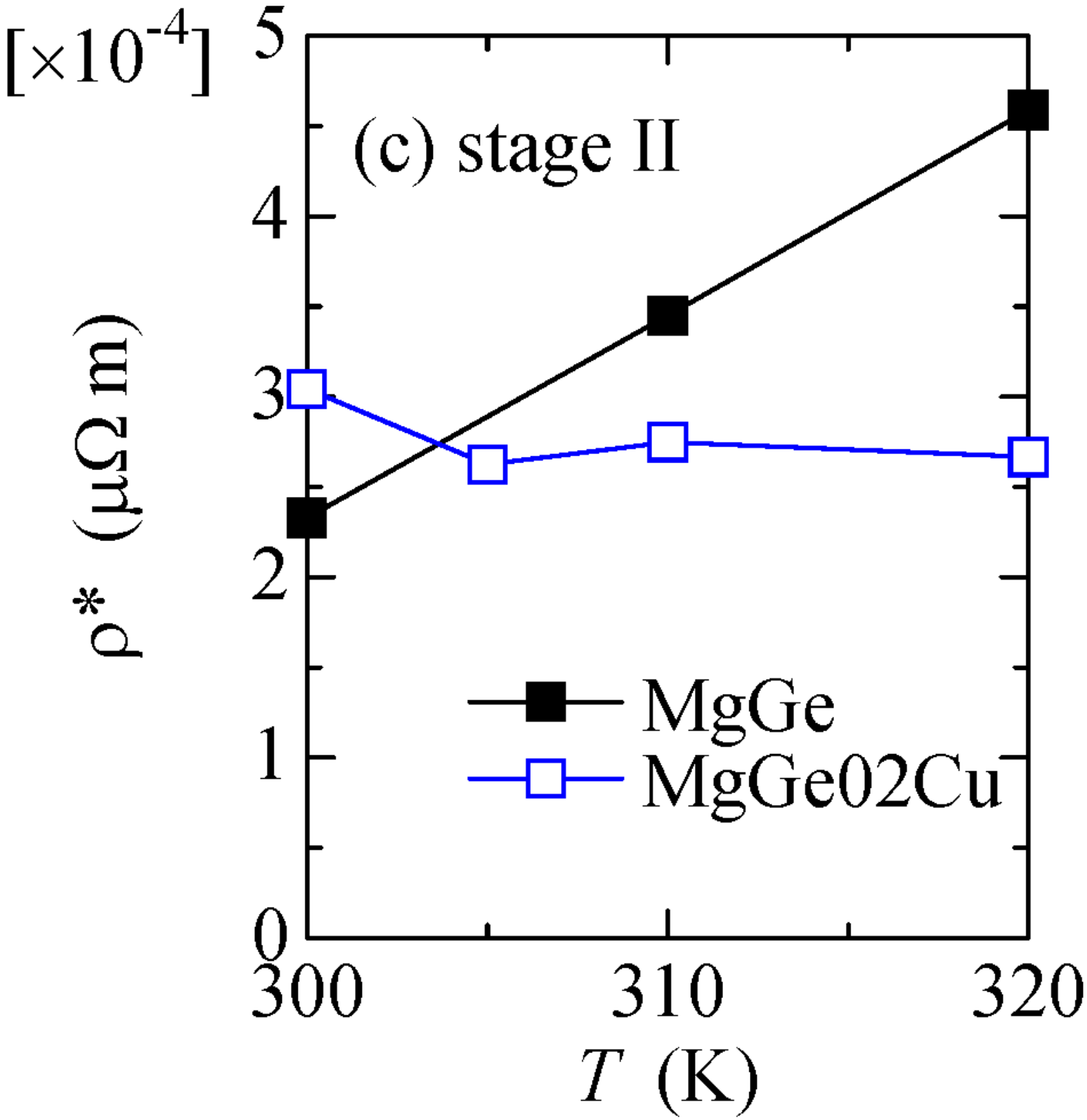
[×10-4]
5
4
3
2
1
0
(c) stage II
ρ* (μΩ m)
MgGe
MgGe02Cu
300
310
320
T (K)

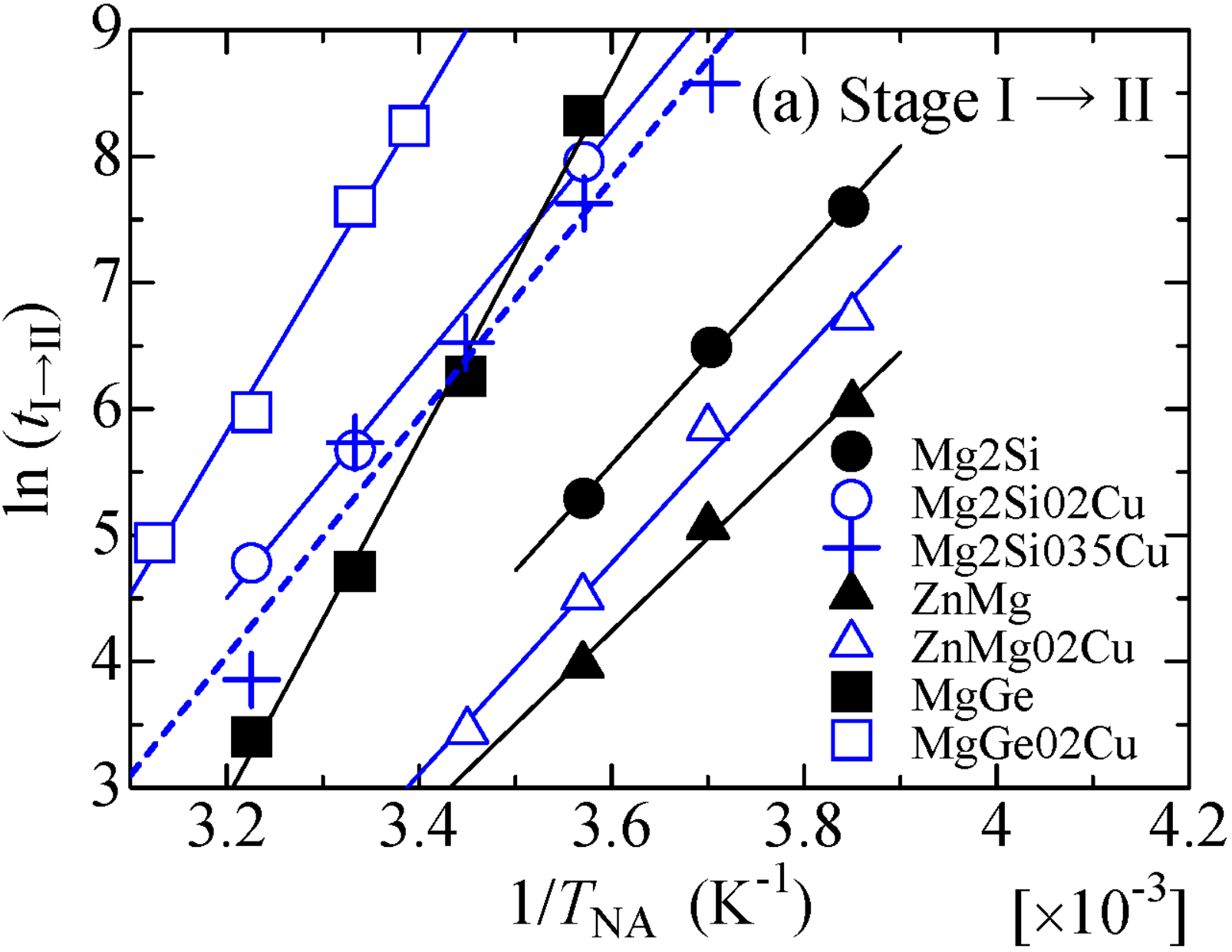
(a) Stage I → II
Mg2Si
Mg2Si02Cu
Mg2Si035Cu
ZnMg
ZnMg02Cu
MgGe
MgGe02Cu
ln ($t_{I\rightarrow II}$)
$1/T_{NA}$ (K^{-1})
[×10^{-3}]
9
8
7
6
5
4
3
3.2
3.4
3.6
3.8
4
4.2

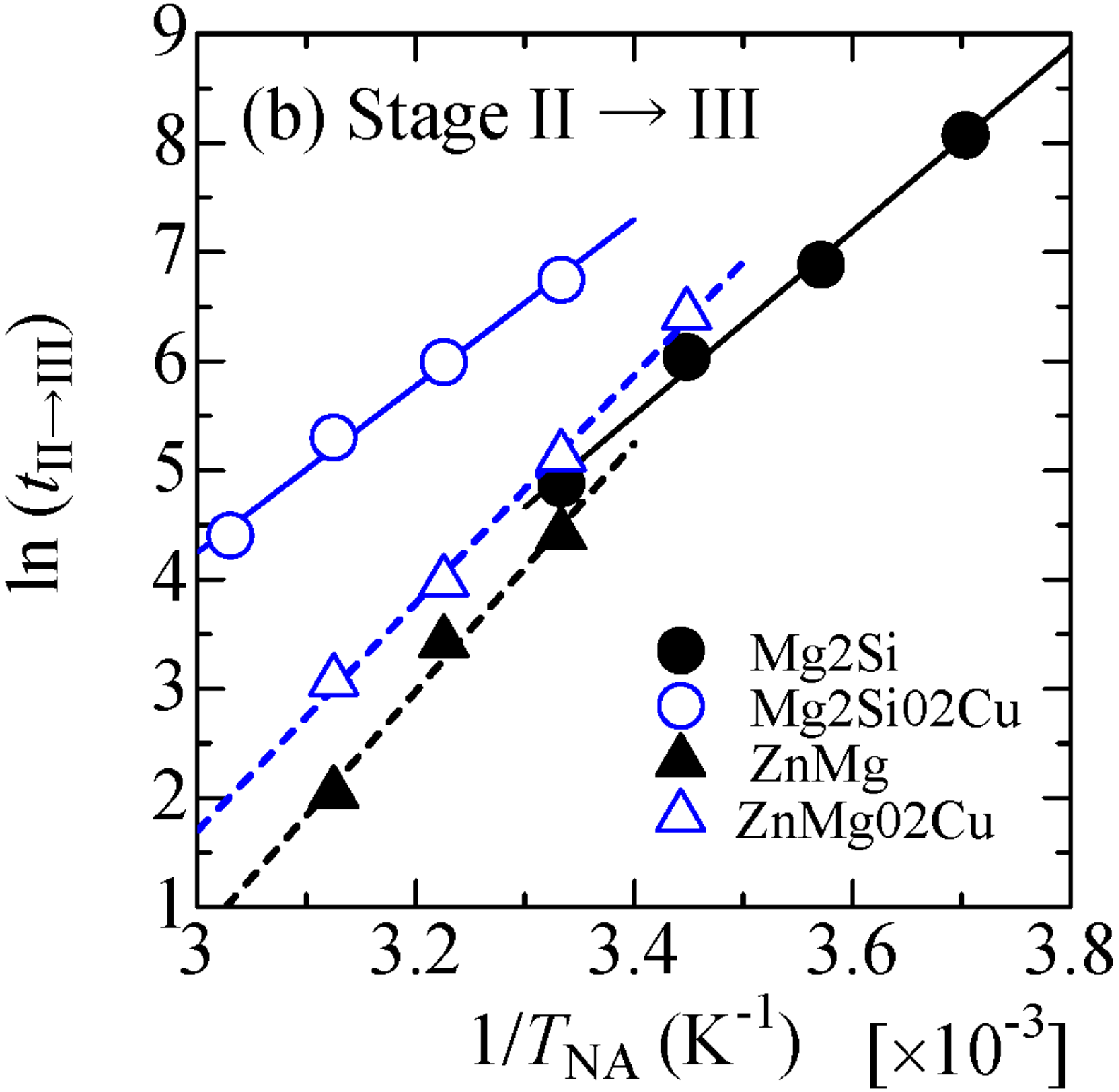
(b) Stage II → III
ln ($t_{II→III}$)
$1/T_{NA}$ (K^{-1}) [×10^{-3}]
Mg2Si
Mg2Si02Cu
ZnMg
ZnMg02Cu
9
8
7
6
5
4
3
2
1
3
3.2
3.4
3.6
3.8

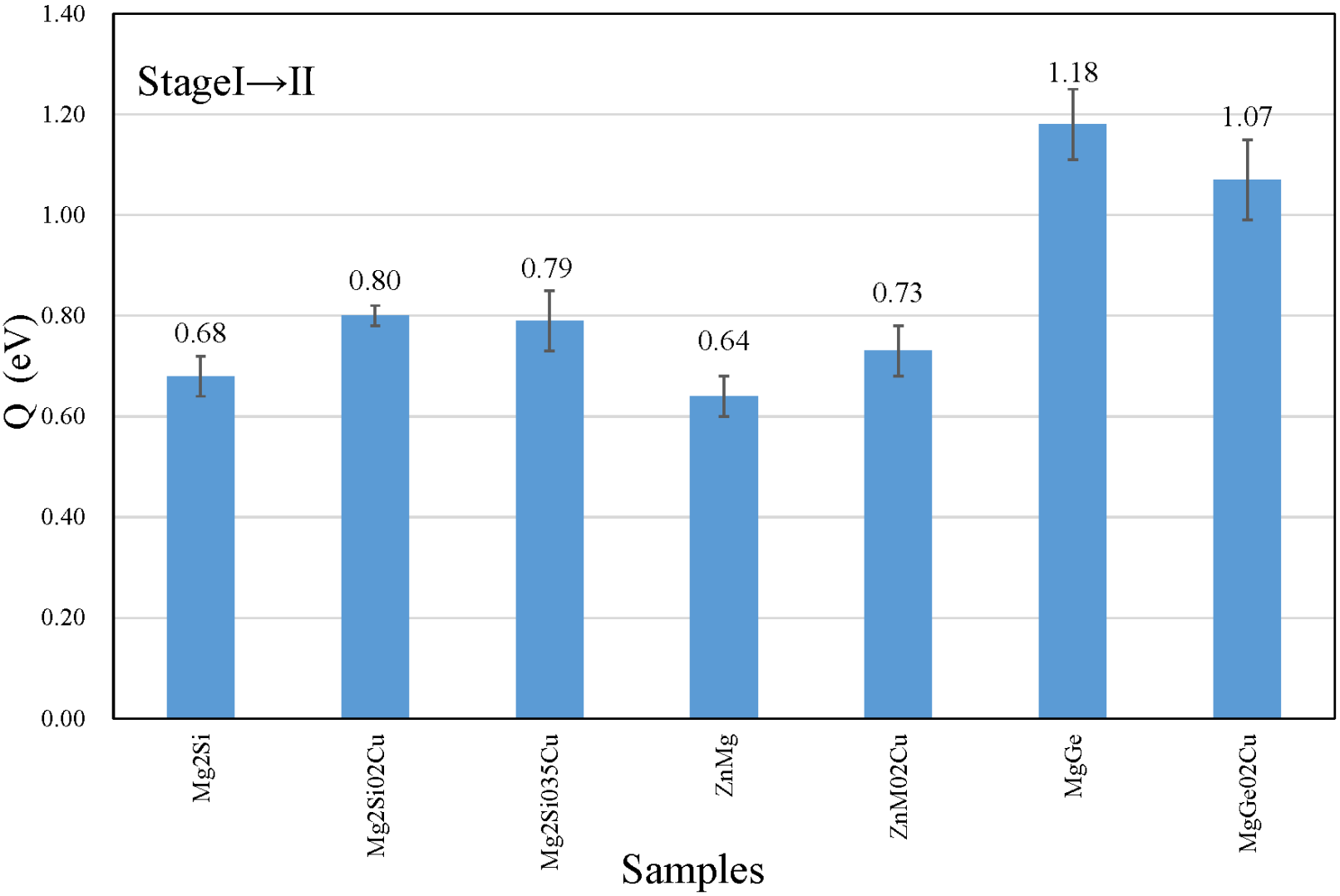
StageI→II
Q (eV)
1.40
1.20
1.00
0.80
0.60
0.40
0.20
0.00
0.68
0.80
0.79
0.64
0.73
1.18
1.07
Mg2Si
Mg2Si02Cu
Mg2Si035Cu
ZnMg
ZnM02Cu
MgGe
MgGe02Cu
Samples

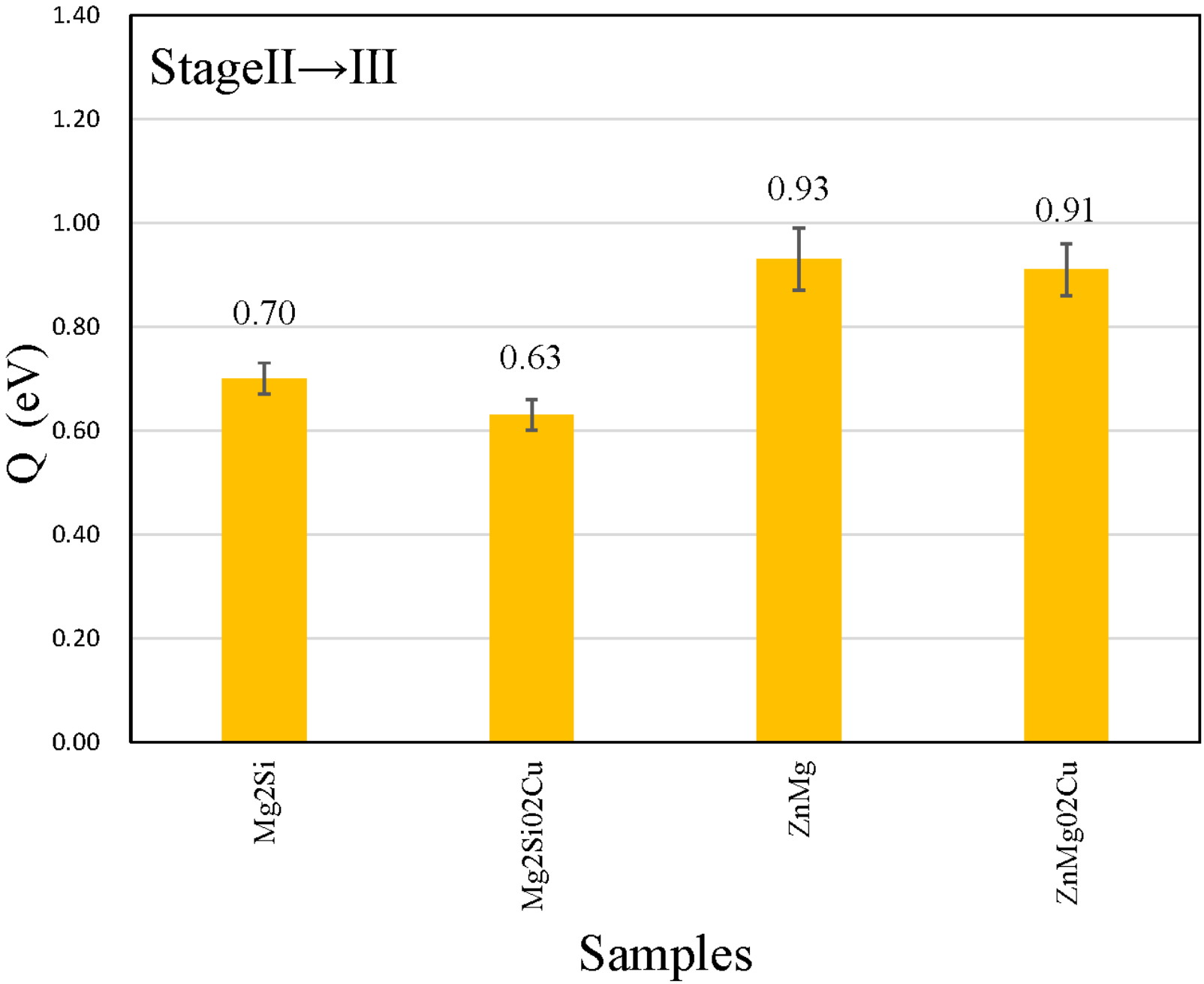
StageII→III
Q (eV)
1.40
1.20
1.00
0.80
0.60
0.40
0.20
0.00
0.70
0.63
0.93
0.91
Mg2Si
Mg2Si02Cu
ZnMg
ZnMg02Cu
Samples